



Università degli Studi di Cagliari

FACOLTÀ DI SCIENZE
Corso di Laurea Magistrale in Informatica

White blood cells segmentation using Vector Field Convolution

Relatore
Prof. Cecilia Di Ruberto

Candidato
Simone Porcu

Anno Accademico 2016-2017

To my grandparents

Abstract

The analysis, counting and classification of white blood cells in automatic way is also an unresolved issue. This automation could be very helpful in medical field, to recognize the kind of pathology that affects a patient. Now the recognize method is completely handmade. In every medical center there is an expert that works hardly to analyse, count and classify the white blood cells in the peripheral blood.

His work is divided in three steps and everyone of these steps is very long. In particular we focused on a particular issue that could affect the optimal result of the work. The analyser after many hours of work due to the fatigue of sight may not sees it as well as before and maybe not see certain particulars affecting cells that could completely change the patient's diagnosis.

Our propose is to create a system that in automatic way is able to do every single step of the blood expert work. We want to do this in order to decrease the time and increase the efficiency of the process.

Our solution is based on a vector field VFC to describe cells edges, without using the active contour model. We choose this approach because we concentrate our work on the segmentation of the white blood cell in overlap position.

At the end we defined a system that is able to recognise the leukocytes from the other cells of the peripheral blood and divide the overlapping leukocytes. Then in conclusion we trying to construct a method able to separate the overlapped cells, that there is the main unresolved issue of the leukocytes segmentation.

Contents

Introduction	1
I Background	5
1 Overview about vector fields and segmentation techniques	7
1.1 The vector field	7
1.2 An overview about Image Segmentation methods	9
1.2.1 Threshold-based techniques	9
1.2.2 Histogram-based techniques	10
1.2.3 Region-based techniques	10
1.2.4 Edge detection technique	10
1.2.5 Watershed technique	11
II About Mean Shift	13
2 Mean shift	15
2.1 Mean shift kernel function	15
2.2 Mean shift definition	16
III About Vector Field Convolution	17
3 Vector field convolution	19
IV A parallel way of using VFC without active contours	21
4 The proposed approach	23
4.1 ALL-IDB blood cell dataset	24
4.2 Mean shift application	27
4.3 The VFC result	27
4.4 External Energy	30
4.4.1 Line functional	30

4.4.2	Edge functional	30
4.4.3	Termination functional	31
4.4.4	External energy result	31
4.5	Combination of two results: the division method	33
4.6	Segmentation with the skeleton function	34
4.7	Cells counting	36
4.7.1	Detection and deletion of small over-segmentation areas	36
4.7.2	Region-Merging	36
V	Results and conclusions	39
5	Experimental results and conclusions	41
5.1	Results	41
5.2	Related works	45
5.3	Conclusions and future works	45
	List of Figures	49
	List of Tables	51
	Bibliography	53

Introduction

This project has been developed under the supervision of Prof. Cecilia Di Ruberto and PhD students Andrea Loddo and Postdoctoral fellow Lorenzo Putzu.

Blood is a body fluid deliver. It contains and transport many of the nutrients substances that the man and the other animals use to live. What we call blood is principally a fluid divided in two elements: blood cells and blood plasma. Normally an individual has around 5 litres of blood. The plasma blood constitutes the 55% of the total fluid. It is mostly water (92% by volume) and contains proteins, glucose, mineral ions, hormones and blood cells themselves.[12] Mainly the cells are red blood cells and white blood cells (WBCs).

In this dissertation we going to focus on WBC especially we will study the shape of these. White blood cells, also called leukocytes, are the cells with the task of controlling the body against both infectious disease and foreign invaders. All leukocytes have a nucleus that distinguishes them by other blood cells, in particular red blood cells and platelets. The generic term leukocytes includes very different cells population: neutrophil, granulocytes, basophilic granulocytes and eosinophilic granulocytes. This set of four categories is defined as polymorphonucleated granulocytes. The other set that includes monocytes and lymphocytes is defined agranulocytes mononuclear 1.

White blood cells segmentation

Segment an image means divide an image in regions of interest. it is used to obtain a more compact image that it is used to extract objects or to analyse an image. More precisely, image segmentation is the process of assigning a label to every pixel in an image such that pixels with the same label share certain visual characteristics. In this case the main feature is to find edges and white blood cells nuclei. At a first look it seems a banal problem, because the we think that every single cell is strongly separated by the others, but obviously it is the best case that we can find. Commonly the microscope photos that we analyse contain noise and in particular the leukocytes overlaps both others



Figure 1: Example of the different kind of leukocytes[10]

leukocytes and red blood cells. For these reasons segment leukocytes is still an unresolved problem. As explain above there are 2 class of leukocytes that are dissimilar by the nuclei shape. This is an high problem because if the solution to find all the white blood cells was based on the search of circular shapes, it is trivial that it will be impossible to recognize a granulocyte from a monocyte.

There are a lot of heuristics and approaches that try to divide white blood cells. This dissertation proposes a new approach of pure segmentation using the Vector Field Convolution, in particular tries to find a division between the overlaps between the cells. The used dataset is ALL-IDB dataset, a public dataset created by the University of Milan. It contains microscopic images of blood samples, specifically designed for the evaluation and the comparison of algorithms for segmentation and image classification.

We choose this vector field because the common practice to extract the features by the images utilizes thresholds, but what happens if the image has a low definition and all the cells overlap each other? Using the vector field to describe the image is possible to transcend from the shape of the features and focus themselves on the points that have a non-uniform virtual field. This technique then considers only the points that describe the edges of the white blood cells. After the image segmentation we obtain an image that contains only segmented leukocytes. With this result we can label every cell without human work.

The first step of the algorithm pre-processes the image in order to overcome the non-linearity of colour distribution inside the image. The literature says that we can overtake this problem using the mean-shift model. The second step applies the Vector Field Convolution on the edge image obtained by the first step, in order to obtain an intensity image of the cells. The third step is focused on the extraction of the angle image in order to obtain the direction of each pixel and to apply to it the Energy function. The fourth step applies the median filtering to the energy image and the angle image and puts them in overlay in order to apply the skeleton function after an opening of the closing of the image. After this step we obtain, joining the skeleton image with the black and white leukocytes image and the Energy image, the first result: the segmentation of the cells and in particular also the segmentation of the cells in overlap. The fifth step merges all the little image's imperfections in order to count the cells and to have a perfect segmentation of the cells.

Chapter 1 introduce a brief explanation about a generic vector field and a summary about the classic segmentation methods, known in literature. Chapter 2 describes Mean Shift theory. Chapter 3 describes Vector Field Convolution and its application to image segmentation. Chapter 4 presents the ALL-IDB dataset and presents the complete realized algorithm. Chapter 5 shows the experimental results, comparison with other methods, conclusions and future aspects.

Part I

Background

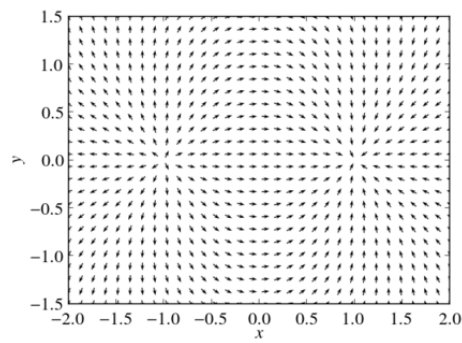
Chapter 1

Overview about vector fields and segmentation techniques

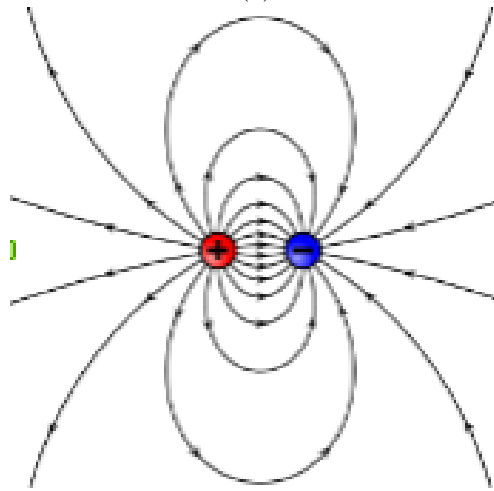
1.1 The vector field

What is a vector field? A vector field is an assignment of a vector to each point in a subset of space. This assignment is the value that will give an orientation to the row that will describe our image. The figure 1.1 represents a vector field flow of an electric dipole in the $x-y$ -plane with $r+ = (-1, 0, 0)$ and $r- = (1, 0, 0)$. All vectors are normalized to the unity. Thus, the plot visualizes the direction of the electric dipole field, but not the field strength. In the negative zone part of the dipole it is possible to see that row of the vector field tries to enter the plane and at the opposite side it's possible to see the exact opposite, that shows the rows exit from the plane. This translates into a flow of rows that is possible to apply to describe the leukocyte's edges.

Active contours, also called snakes, are curves that move inside the image following the energy of the field. There are two kinds of forces, one internal and another external. Combining these two it is possible to create a curve that follows constraints provided by the forces. The internal and external forces are defined so that the snake will conform to an object boundary or other desired features within an image. Snakes are widely used in many applications, including edge detection, shape modelling and segmentation. There are two general types of active contour models in the literature today: parametric active contours and geometric active contours. Typically, the curves are drawn toward the edges by potential forces, which are defined to be the negative gradient of a potential function. Additional forces, such as pressure forces, together with the potential forces comprise the external forces. There are also internal forces designed to hold the curve together and to keep it from bending too much. There are two levels of difficulties with active contour algorithms. First, the initial contour must be close to the true boundary or else it will



(a)



(b)

Figure 1.1: (a) Dipole electric field, (b) Electric dipole

likely converge to the wrong result. The second problem is that active contours have difficulties progressing into concave boundary regions. Although many methods such as multi resolution methods, pressure forces, distance potential forces, control points, and using solenoidal external fields have been proposed they either solve one problem or solve both but creating new difficulties. For example, multi resolution methods have addressed the issue of initialization, but specifying how the snake should move across different resolutions remains problematic. Another example is the pressure forces, which can push an active contour into boundary concavities, but cannot be too strong or “weak” edges will be overwhelmed. But how works a snake if the objects to segment are overlapped? Snakes are able to find all the external edges of the object but in this case the edge can be consider an internal part of the object. With the active contours it is impossible segment the overlapped cells because the snake cannot enter inside the cell region. For these reasons we have used our virtual field following another lecture key. We use it only to exalt the edges of the cells in order to extract them.

1.2 An overview about Image Segmentation methods

When we talking about segmentation we introduce a technique for partitioning the image into subregions. The most five famous techniques to develop an image segmentation are described below:

1. threshold-based;
2. histogram-based;
3. region-based;
4. edge detection;
5. watershed transformation.

1.2.1 Threshold-based techniques

Thresholding is the simplest segmentation method. The pixels are partitioned depending on their intensity value generally used with gray scale images $f(x, y)$. When the threshold is applied on gray scale images the final target is separate the foreground by the background. The first one contains only the element of interest and the second one contains all the rest of the image. The global threshold value T is the 'breaking point' of the image. After an analysis of the image, the value T is used to understand if, a pixel of the image belongs to the foreground $f(x, y) > T$ or to the background $f(x, y) < T$.[5]

1.2.2 Histogram-based techniques

An important class of point operations is based upon the manipulation of an image histogram or a region histogram. It uses the histogram to select the gray levels for grouping pixels into regions. The image is composed by the foreground and the background. Generally the background occupies most of the image and for this reason its gray level will be a large peak in the histogram. The object of the image as opposed to the background is a smaller peak in the histogram. Then we can choose a threshold point in the valley between the two peaks and threshold the image.

1.2.3 Region-based techniques

Differently from the other two techniques described before, the region-based segmentation is a technique for determining the region directly. Initially set of point of interest are created. Starting from these points other regions grow up if neighbouring pixels have similar properties as that of point of interest. In region splitting and merging, an image is subdivided into different regions and then either merged and split. As first step the image is split into four disjoint quadrants, then merges any adjacent regions, which satisfy the imposed constraints. Like a loop we repeat splitting of regions and merging till no further merging or splitting is possible. Image regions are implemented with the help of quad trees. The basic formulation is:

- (a) $\bigcup_{i=1}^n R_i = R$.
- (b) R_i is a connected region, $i = 1, 2, \dots, n$
- (c) $R_i \cap R_j = \emptyset$
- (d) $P(R_i) = TRUE$ for $i = 1, 2, \dots, n$.
- (e) $P(R_i \cup R_j) = FALSE$ for any adjacent region R_i and R_j

where $P(R_i)$ is a logical predicate defined over the points in set R_i and \emptyset is the null set. (a) Means that the segmentation must be complete that is, every pixel must be in a region. (b) Requires that points in a region must be connected in some predefined sense. (c) Indicates that the regions must be disjoint. (d) Deals with the properties that must be satisfied by the pixels in a segmented region. For example, $P(R_i) = TRUE$ if all pixels in R_i have the same gray-scale. (e) Indicates that region R_i and R_j are different in the sense of predicate P . [13]

1.2.4 Edge detection technique

Edge detection includes a variety of mathematical methods that aim at identifying points in a digital image at which the image brightness changes sharply or, more formally, has discontinuities. The points at which image brightness changes sharply are typically organized into a set of curved line segments termed edges. The same problem of finding discontinuities in one-dimensional

signals is known as step detection and the problem of finding signal discontinuities over time is known as change detection. Edge detection is a fundamental tool in image processing, machine vision and computer vision, particularly in the areas of feature detection and feature extraction.[4] Is possible to divide edges in two different set: intensity edges and texture edges. The first one includes steps and roofs. The texture edges set include all the regions that are invariant to the luminance conditions. Then to obtain a continuous edge is necessary a function of edge linking. The most famous edge detection algorithms are Sobel, Prewitt, log, zero-cross, Roberts, Canny.

1.2.5 Watershed technique

This function considers the magnitude of the image like a topographic surface. We can consider it like an high ground of a gray-scale image, where the gray level of a pixel shows its height in the high ground. In proximity of the watershed lines the pixels have an high magnitude intensity. The water is put inside the regions enclosed by the watershed lines. As is possible to understand from these lines we are talking about a local minimum. We said it because for each region we find the local minimum and we fill it with the water. The result is composed only by the max-points of the image.

Next chapter illustrates, in detail, how we use the Mean Shift segmentation technique and the use of its result with the VFC.

Part II

About Mean Shift

Chapter 2

Mean shift

Mean Shift technique was originally proposed in 1975 by Fukunaga and Hostetler [6], then adapted by Cheng [15] and generalized by Cheng, Comaniciu and Meer [2] for image analysis purposes. It is a no-parametric method for locating the modes of a density function in discrete data sampled. It is an iterative method that starts with an initial estimate x .

2.1 Mean shift kernel function

Given a kernel function $K(x_i - x)$, as the function that determines the weight nearby points to re-estimate the mean. The kernel function has to respect the following constraints:

$$\int R^d \phi(x) = 1 \quad (2.1)$$

$$\phi(x) \leq 0 \quad (2.2)$$

The literature talks about some different kernel definitions, but typically mean-shift uses the Gaussian kernel or Epanechnikov kernel, respectively explained below:

$$\phi(x) = e^{-\frac{x^2}{2\sigma^2}} \quad (2.3)$$

$$K(x) = \begin{cases} \frac{3}{4}(1 - x^2) & \text{if } |x| \leq 1 \\ 0 & \text{else} \end{cases} \quad (2.4)$$

Known as KDE, Kernel Density Estimation, in statistics is considered a non-parametric way to estimate the probability density function of a random variable. KDE is a data smoothing problem where inferences about the population are based on a finite data sample. When we work in the field of signal processing and econometrics it is termed the Parzen-Rosenblatt window method.

Given an unknown density f of a distribution X , we want to estimate the shape of this function f . Its kernel density estimator is

$$\hat{f}_h(x) = \frac{1}{n} \sum_{i=1}^n K_h(x - x_i) = \frac{1}{nh} \sum_{i=1}^n K\left(\frac{x - x_i}{h}\right) \quad (2.5)$$

where the kernel $K(x)$ is a scalar function.

2.2 Mean shift definition

Define a d-variate kernel function $K(y)$ to be a search window; if it is symmetric:

$$K(y) = ck(\|y\|^2) \quad (2.6)$$

where c is the normalization constant, $k(s)$ is a symmetric univariate kernel which that it is the profile of $K(y)$ if $s \geq 0$ and y is the center location of the search window. Calculating the location of the centroid of the search window we obtain a vector of the differences between the local mean and the centre of the window

$$m_k(x) = y_{centroid} - y \quad (2.7)$$

Defined ξ as an arbitrary small value, indicating a threshold, if

$$\|m_k(y)\|^2 \geq \xi \quad (2.8)$$

the search window can be moved iteratively, because it means that it has not yet reached the convergence, that is the value in which we can stop computing the Mean Shift value.

As we said previously this is an iterative algorithm, then the search window can be moved iteratively, because it means that it has not find the convergence. The convergence is simply the value in which we can stop computing the mean shift value. Now is possible to define the other centre of the search window and start again the process.

In order to use this function the user has to choose three input parameters:

1. h_s . Spatial bandwidth value in which the Mean Shift will be computed. It indicates the maximum radius within the pixels are considered for the computation of the Mean Shift value;
2. h_r . Colour bandwidth value. It indicates the maximum colour difference between actual pixel value and the pixel taken for the computation. If the difference is greater than h_r , the pixel will not be considered for the computation of new value;
3. th . Threshold value. It represents the parameter ξ . When this value is reached, the algorithm terminates.

Part III

About Vector Field Convolution

Chapter 3

Vector field convolution

The vector field convolution is a snake external force created by Bing Li and S.T. Acton.

Convolving a vector field with the edge of the map derived from the image you get an external force, the VFC. Active contours using the VFC external force are called VFC snakes. Like the GVF [14] snakes instead of being formulated using the standard energy minimization framework, VFC snakes are constructed from a state of equilibrium between the forces. The VFC snakes besides having a wide capture range and the ability to capture the concavities, are better resistant to noise image, have the ability to adapt the force field and reduce drastically the computational cost. Before to explain the VFC it is right to explain the vector field kernel

$$k(x, y) = m(x, y)n(x, y) \quad (3.1)$$

where n is the unit vector that points to the origin of the kernel

$$n(x, y) = \left[\frac{-x}{r}, \frac{-y}{r} \right] \quad (3.2)$$

and m is the magnitude of the vector . The authors of the VFC implemented two kinds of magnitude. If we consider the origin as the point of interest, this vector field kernel has the desirable property that a free particle placed in the field is able to move to the point of interest. The external force that works in the VFC is defined in this way:

$$f_{vfc}(x, y) = u_{vfc}(x, y), v_{vfc}(x, y) \quad (3.3)$$

Since the map of the edge is non-negative and is wider near the edges of the image, the edges act to a greater extent on the VFC than homogeneous regions. Therefore, the free particles of homogeneous regions will be attracted to the edges. If we present the vector field kernel using a complex-valued range, the VFC is just the filtering result of the edge map, which does not depend on the

origin of the kernel. The VFC field highly depends on the magnitude of the vector field kernel . The field VFC has the magnitude directly proportional to the vector field kernel (x, y) . Knowing that the figure of interest has less influence on the particles away from it, the magnitude must be expressed as a positive function decreasing with respect to the distance of the origin. Below we propose two types of magnitude functions, given as

$$m_1(x, y) = (r + \epsilon)^{-\gamma} \quad (3.4)$$

$$m_2(x, y) = \exp(-r^2 \zeta^2) \quad (3.5)$$

where γ and ζ are positive parameters to control the decrease, ϵ is a small positive constant to prevent division by zero at the origin. $m_1(x, y)$ is inspired by Newton's law of universal gravitation in physics. Furthermore, the pixels in the edge map can be considered as objects of mass proportional to the strength of the edges and the field VFC would be the gravitational field generated by all objects. The influence of the figure of interest increases as γ decreases. In practice γ usually ranges from 1.5 to 3 for most images. $m_2(x, y)$ is a Gaussian shape function, where ζ can be viewed as the standard deviation. The influence of the figure of interest increases as ζ increases. In general, the influence of the figure of interest should be increased (decrease or increase) as the signal-to-noise ratio is decreased.[1]

Part IV

A parallel way of using VFC without active contours

Chapter 4

The proposed approach

In the thesis we propose a new and innovative system for the white blood cells segmentation and counting based on the Vector Field Convolution.

In the diagram 4.1 the scheme of the proposed system is showed. In the first phase we acquire the image containing the cells. In the second step the mean-shift method is applied in order to obtain a better image for the segmentation. In the third step we apply the VFC method in order to obtain the intensity image. The fourth step transform the intensity image in a grade image where each pixel has a specific direction. The fifth and the sixth steps are parallels. In the fifth step we calculate the external energy and the distance transform on the grade image. In the sixth step the median filter is applied on the results of the fifth step. The seventh step shows the overlay between the two results of the sixth step in order to detect only the leukocytes. The eighth step applies the skeleton method in order to do an initial segmentation. The ninth step applies the region merging function to segment and finally count the cells in the image.

As we can see in literature, the main approach used to resolve the overlap problem is using the watershed transform [9]. In figure (4.2a) there is an example of the watershed transform. Taken in input the image of the two overlapped circles, we calculate the distance transform, or in other words we calculate the Euclidean distance transform of the binary image BW. For each pixel in BW, the distance transform assigns a number that is the distance between that pixel and the nearest non-zero pixel of BW (4.2b). Giving the distance transform result to the watershed algorithm we obtain a division between circles because the watershed transform finds "catchment basins" or "watershed ridge lines" in an image by treating it as a surface where light pixels represent high elevations and dark pixels represent low elevations (4.2c). This is an ideal case to analyse. But when we work with the overlapping between cells the result of the division by watershed transform is not optimal like

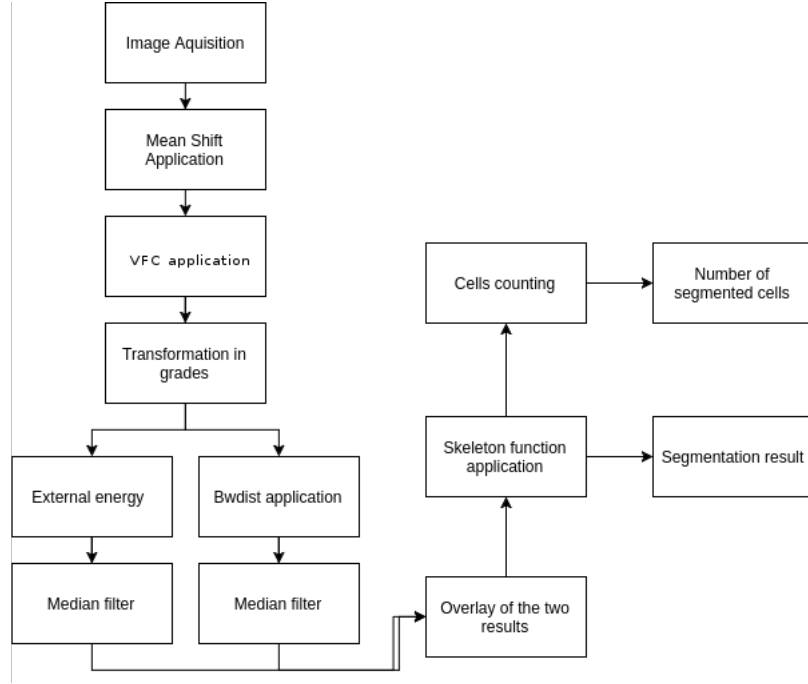


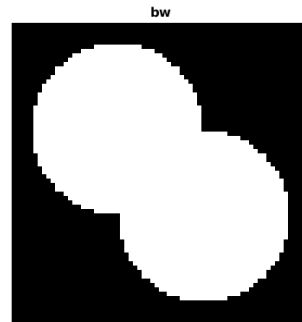
Figure 4.1: Method diagram representation

the example 4.2. Probably the cause derives from the low definition of the figures and especially the shape of the cells. Here there is an example of what happens when we try to divide three cells in overlap (4.3). As it is possible to see, this method produces a no-realistic separation of the cells. For this reason we study a different method that in automatic way produces a realistic division of the cells. Starting from the resulting image after the application of the mean shift algorithm, we based our implementation using principally the output of the VFC field, the image relative to the External energy of the image to describe the edges, the median filter, the skeleton method and the region-merging function.

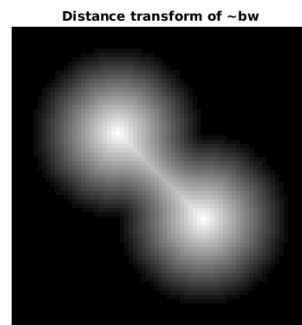
The proposed system has been tested on images belonging to a public dataset, the ALL-IDB blood cell dataset [7].

4.1 ALL-IDB blood cell dataset

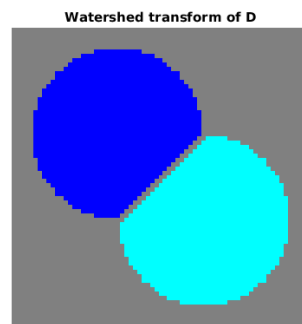
The images of the dataset have been captured with an optical laboratory microscope coupled with a Canon PowerShot G5 camera. All images are in JPG format with 24-bit colour depth. The first 33 have 1712×1368 resolution, the remaining have 2592×1944 resolution. The images are taken with different



(a)

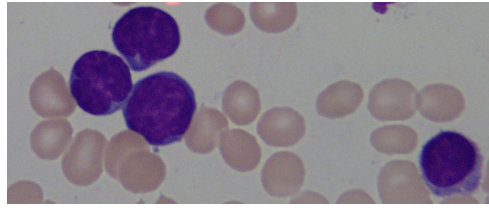


(b)



(c)

Figure 4.2: (a) Example of two circle in overlap, (b) Distance transform, (c) Watershed result



(a)



(b)

Figure 4.3: (a) Original leukocytes image, (b) Watershed transform applied to three cells in overlap

Characteristic	ALL-IDB1	ALL-IDB2
Images	109	260
Max resolution	2592x1944	257x257
Elements	39000	260
Candidate Lymphoblasts	510	130

Table 4.1: Characteristics of the dataset. Images acquisition has been performed with a Canon PowerShot G5. Magnification of microscope goes from 300 to 500. The image format of the ALL- IDB1 folder images is JPG, ALL-IDB2 images have TIF format. The colour is 24 bit depth.

magnifications of the microscope ranging from 300 to 500 which brings the colour differences that we managed grouping the images with same brightness characteristics together. The ALL-IDB database has two distinct folders (ALL-IDB1 and ALL-IDB2).

The table 4.1 shows a little description about the images. The IDB1 set can be used for testing segmentation capability of algorithms. This dataset is composed of 108 images collected during September, 2005. It contains about 39000 blood elements, where the lymphocytes have been labelled by expert oncologists.[11] The IDB2 set has been designed for testing the performances of classification systems. The ALL-IDB2 version 1.0 is a collection of cropped area of interest of normal and blast cells that belongs to the ALL-IDB1 dataset. ALL-IDB2 images have similar gray level properties to the images of the ALL-IDB1, except the image dimensions.[11] For our work we consider changed only normal type of leukocytes and we focused principally on the images where

is present an overlap between the white blood cells.

4.2 Mean shift application

In order to resolve the illumination problems and to obtain a good visualization of the Wright-Giemsa stain cells we use the mean shift function. To obtain an acceptable result it should be necessary an image preprocessing, but using the bandwidth parameters and the threshold parameter of the mean shift function we can obtain the same result. For our work we used h_s (bandwidth of the spatial kernel) = 4, h_r (colour bandwidth) = 4 and the threshold $th = 0.25$. The result obtained by changing these parameters is not so significant in order to obtain a good final result, then is preferable use an image with a little bit definition but obtained in a very short time (2 seconds for cropped images and 40 seconds for the entire images). To understand what are the differences in the image when we apply the mean shift procedure, is appropriate do a comparison between the images before and after the application of the method (4.4). The resulting image is very helpful to calculate the edge map that will give as parameter to the VFC function.

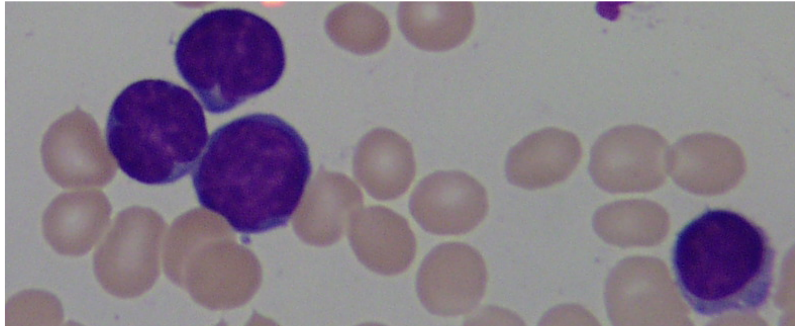
4.3 The VFC result

The VFC uses the two components of the external force $u_{vfc}(x, y), v_{vfc}(x, y)$ to describe the field of the image and its magnitude. Our purpose is find an image using these two components that describes all the leukocytes edges taking an accurate look on the edges in overlap and in clump. The first step then is extract the right component and the left component by the VFC field.

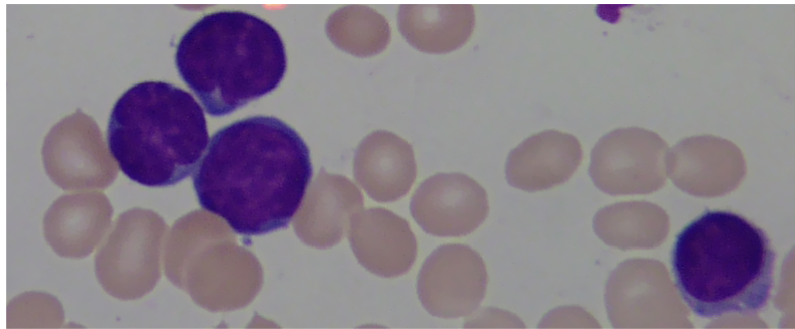
$$u_{vfc} = ExtF(x) / \sqrt{ExtF(x)^2 + ExtF(y)^2} \quad (4.1)$$

$$v_{vfc} = ExtF(y) / \sqrt{ExtF(x)^2 + ExtF(y)^2} \quad (4.2)$$

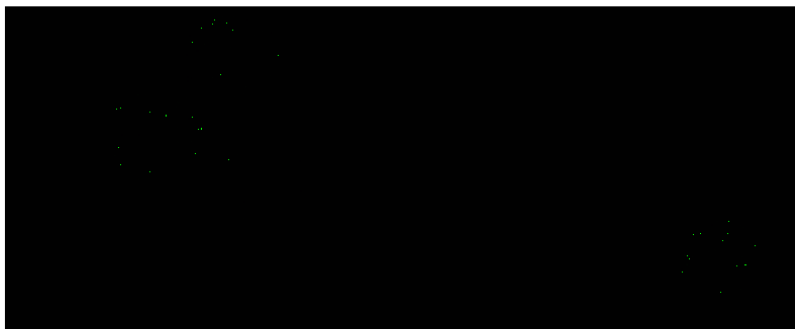
ExtF is the External force of the field. Now we have only an intensity image, but to understand how the field moves in the space we have to transform these two component u and v in grades. We want to understand the direction of every pixel in the figure especially the pixels that describe edges of cells. It is possible to convert the two components in degrees using the *atan2d* function 4.5. In order to delete all the uniform part of the figure and put in exalt the edges we use a mediand filter using the function *ordfilt2* searching the 18th element of the $5 * 5$ mask (4.6).



(a)



(b)



(c)

Figure 4.4: (a) Original image, (b) Mean-shift result, (c) Difference between mean-shift image and original image

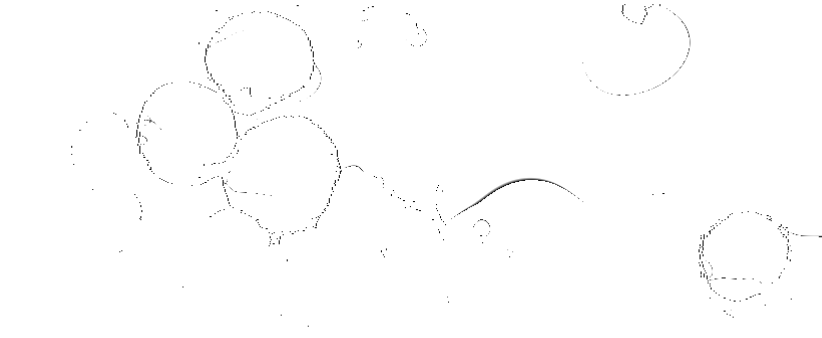


Figure 4.5: Degrees image

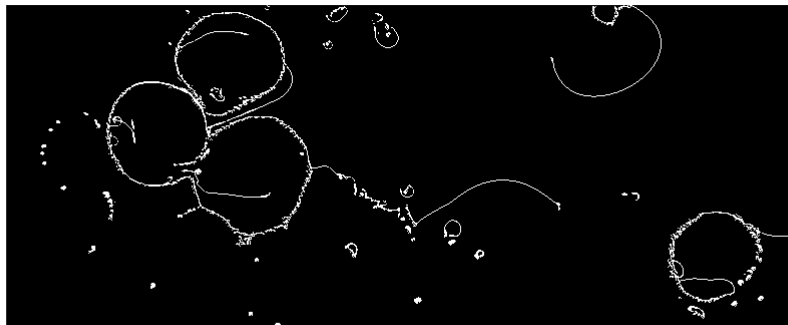


Figure 4.6: Median filter on degrees image



Figure 4.7: Bwdist applied on degrees image

4.4 External Energy

As it is possible to see in the result 4.5, there are a lot of points that are artefacts created by the field. For these reason we used the *bwdist* function to assign a number that it is the distance between each pixel and the nearest no-zero pixel of the image. This trick is very useful because it reduces the entropy of the image, focusing only on the shape of the leukocytes (4.7). But we have still the same problem. In the image there are trace of the red blood cells, then we had to find a method to isolate only the leukocytes. We started using the external energy of the image. For an image $I(x, y)$ all the lines, edges and terminal points the general formulation of the Energy of the image is

$$E_{image} = w_{line}E_{line} + w_{edge}E_{edge} + w_{term}E_{term} \quad (4.3)$$

where w_{line} , w_{edge} , w_{term} are weights of the features.

4.4.1 Line functional

The line functional or in other terms the intensity of the image is in a nutshell the attracted value of the dark lines to the light line. Is possible choose this attraction putting a positive or negative sign before the force that this attraction has to be.

$$E_{line} = filter(I(x, y)) \quad (4.4)$$

4.4.2 Edge functional

The edge functional bases its work on the image gradient.

$$E_{edge} = -|\nabla I(x, y)|^2 \quad (4.5)$$

It's very useful because when we try to analyse the feature of the image, we work with maxims and minims. With this formula we can avoid the local minima that are not object of interest. The energy functional using scale space continuation is

$$E_{edge} = - \left| G_{\sigma} * \nabla^2 I \right|^2 \quad (4.6)$$

where G_{σ} is a Gaussian with standard deviation σ .

4.4.3 Termination functional

The curvature of the lines in a image is utilized to detect corners and terminations. Put

$$C(x, y) = G_{\sigma} * I(x, y) \quad (4.7)$$

with a gradient angle

$$\theta = \arctan \left(\frac{C_y}{C_x} \right), \quad (4.8)$$

unit vectors that move along the gradient direction

$$\mathbf{n} = (\cos \theta, \sin \theta) \quad (4.9)$$

and unit vectors perpendicular to the gradient direction

$$\mathbf{n}_{\perp} = (-\sin \theta, \cos \theta). \quad (4.10)$$

With these 4 equations we can describe the termination functional of energy as follow

$$E_{term} = \frac{\partial \theta}{\partial n_{\perp}} = \frac{\partial^2 C / \partial^2 n_{\perp}}{\partial C / \partial n} = \frac{C_{yy}C_x^2 - 2C_{xy}C_xC_y + C_{xx}C_y^2}{(C_x^2 + C_y^2)^{3/2}} \quad (4.11)$$

4.4.4 External energy result

Now we have only to specify the value of each parameter as explained above. To obtain the desired outcome we did some empirical experiments, obtaining the best result with $Wedge = 8$, $Wline = -8$ and $Wterm = 0$. This result (4.8) permit us to extract only the leukocytes part of the image using some analysis image exploit (4.9).

In order to delete all the uniform part of the figure and put in exalt the edges we use a mediand filter using the function *ordfilt2* searching the 18th element of the $5 * 5$ mask 4.10.



Figure 4.8: External energy result



Figure 4.9: External energy image of leukocytes without red blood cells

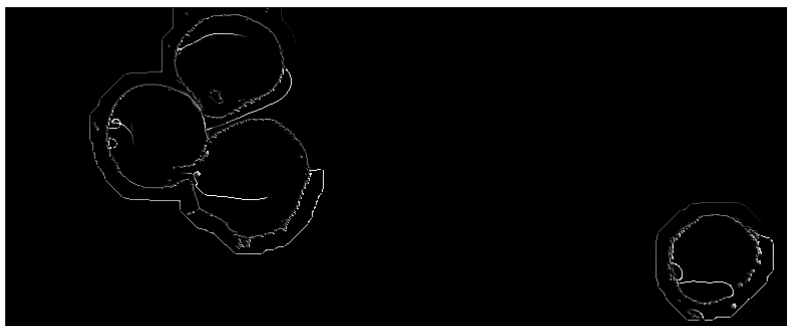


Figure 4.10: Edges and region

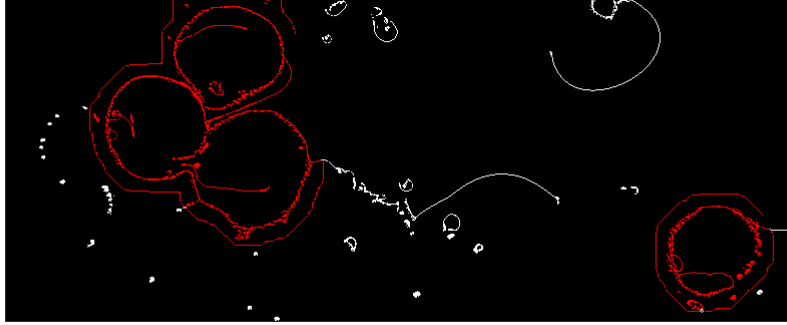


Figure 4.11: Overlay of figures 4.6 and 4.10

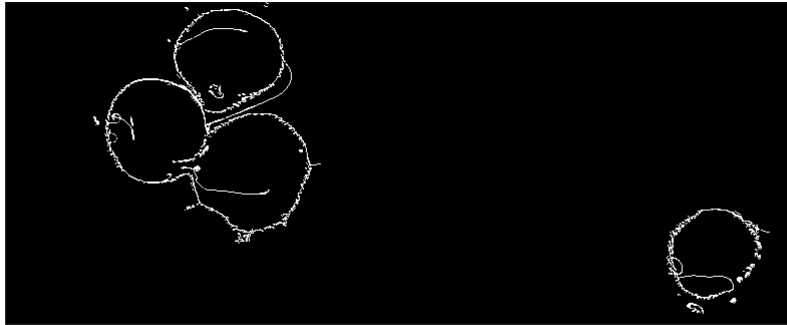


Figure 4.12: Only leukocytes edges

4.5 Combination of two results: the division method

The two obtained results seem in no-correlation, but the skill of this segmentation lives in this passage. Using the overlay function we search all the points in overlay between the median filter application on the degrees image and the edges region, using the red color to isolate the leukocytes region 4.11. We choose to use the red color, because by isolating only the red component of the image we can obtain an image that contains only the leukocytes regions. The result of this task is visible in the image 4.12

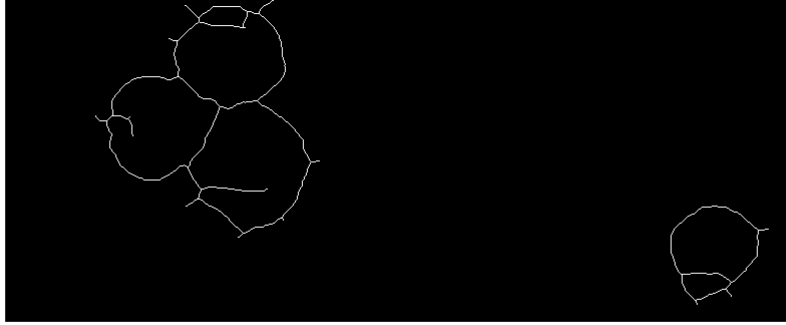


Figure 4.13: Skeleton of leukocytes with irregular branches

4.6 Segmentation with the skeleton function

Starting from the image containing only the edges we have to connect every single white point to the nearest in order to get a connected boundary of the objects. To do this task we use the function *imdilate* to dilate all the white dots with a diamond structural element with the size of 6 pixels. After this step we apply the closing of the opening with two disk respectively of the size 3 and 4 pixels. Now we can apply the skeleton function or the thinning of the edges. To do this passage we use the Matlab function *bwmorph* that it's not the best function to do this but is the faster one. We try another skeleton external function written by N. Howe that is very interesting because has a precision to compute the skeleton of the image that is very impressive, but because the Pc latency we can't use the last one function. After the skeleton application we obtain an image that contains some spurious branches (4.13).

To solve this problem is possible to use the Matlab function *bwmorph* to prune the spurious branches, but in this case the function doesn't work very well. For this reason we implement an alternative code to resolve the problem. Our code is like a parser that for each point sees if it is a part of a closed circle or not. If it's not a part of a loop the code deletes this point. In a nutshell we save only the point that stay in a 'road' with the starting point and the end point coincident. Below you can read a snippet of pruning code.

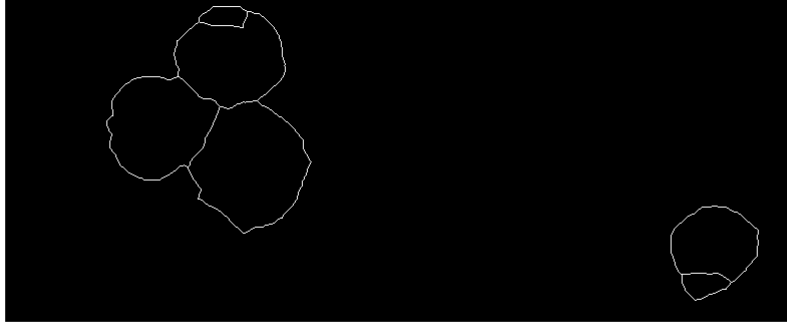


Figure 4.14: Skeleton of leukocytes with no spurious branches

```

B = branchpoints;
E = endpoints;
[y,x] = Image;
Dmask = false(size(skel));
    for k = 1:numel(x)
        D = bwdistgeodesic(skel,x(k),y(k));
        distanceToBranchPt = min(D(B));
        Dmask(D < distanceToBranchPt) = true;
    end
skelD = skel - Dmask;

```

The result that we obtain from the skeleton application is a summary work, indeed we obtain an over-segmentation as is viewable from the image 4.14. This over-segmentation isn't good for the correct visualization of leukocytes, but gives us a starting point to improve the solution and to obtain a better result. Then we try to combine the various result to obtain a segmentation that was similar to the original image. First of all we close all the holes that are inside the image, to obtain a sort of black and white mask. Another fundamental step is summing the skeleton image with the mask. Doing this step we can separate the foreground by the background. Now we can use for the last time the map of edges that we used to calculate the VFC field. Doing an opening with a disk structural element with radius of 6 pixels and summing it with the image of leukocytes in foreground we can extract all connected components using the function *bwareafilt*. We do this because this function extracts all connected components (objects) from a binary image where the area is in range, producing the first segmented image of the leukocytes (4.15).

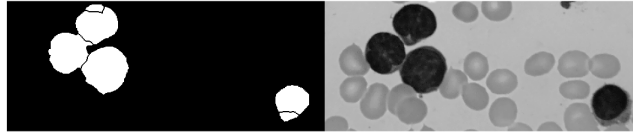


Figure 4.15: Final leukocytes segmentation

4.7 Cells counting

4.7.1 Detection and deletion of small over-segmentation areas

To understand if all that we did had a sense, we have to do a counting of the cells. Because the images have a low definition we can found an over segmentation inside the cells, but is easy to overcome this problem if we do not consider the little regions that are inside the image. This was our first approach in order to obtain a good counting. Then if we delete all the regions that are less than an upperbound we can have the exact number of leukocytes inside the image. We do this using the following snippet code

```
CC = bwconncomp(BW2,8);
numPixels = cellfun(@numel,CC.PixelIdxList);
[~,idx] = min(numPixels);

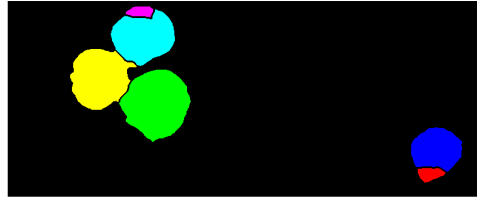
while min(numPixels) < cellsize/2
    BW2(CC.PixelIdxList{idx}) = 0;
    CC = bwconncomp(BW2,8);
    numPixels = cellfun(@numel,CC.PixelIdxList);
    [~,idx] = min(numPixels);
end
[labeledImage, numberOfObject] = bwlabel(BW2);
```

The resulting image of this consider only the regions that are of the same size as the nucleus or bigger.

This result is not really good in order to have a good segmentation. But it gives us the idea to implement a region-merging function.

4.7.2 Region-Merging

In order to obtain a merge of the areas we have followed this approach. As first step we separate in two different images the small areas and the big



(a)



(b)

Figure 4.16: (a) All the regions, (b) Only big regions

areas, because we want to know about every small area to which of the big areas it belongs. The threshold used to create these two different images is the medium of the biggest region that there is in the image. To know it we use the minimum distance between the centroids of one small area and all centroids of the big areas. Then as soon as we labelled every area and we calculated all the centroids we can know what are the areas with minimum distance using the Euclidean distance formula. Now is possible to isolate the two areas 4.17. To merge them we use the function *imclose* with a disk element with 5 of radius 4.18. Now we can join this result with the image with over-segmentations using the mathematics union operator 4.19.

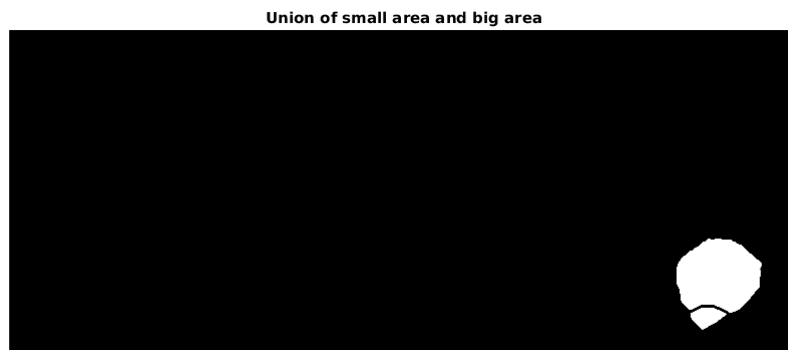


Figure 4.17: Union of two different areas

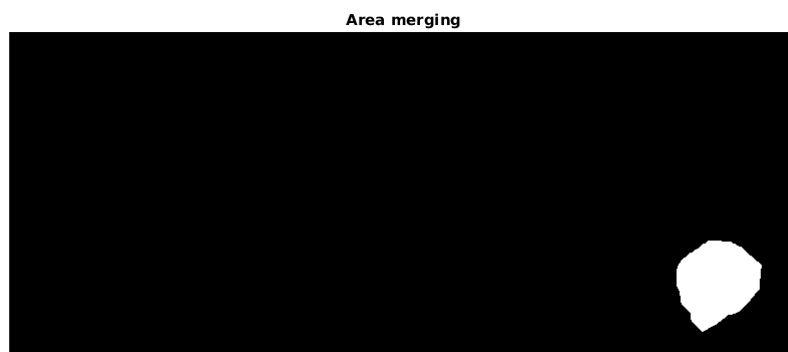


Figure 4.18: Merge of two areas

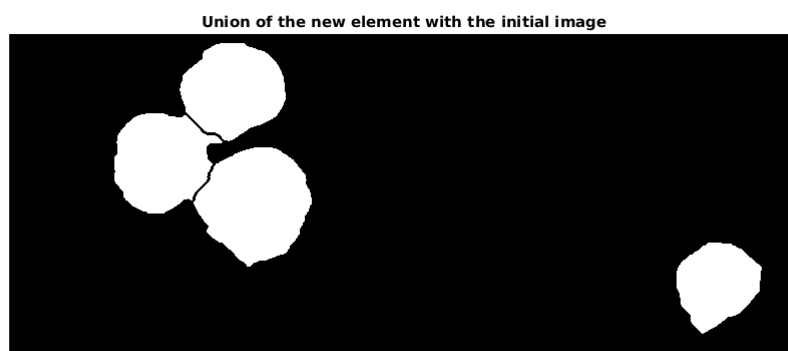


Figure 4.19: Union of initial image and new area

Part V

Results and conclusions

Chapter 5

Experimental results and conclusions

5.1 Results

Our propose in a nutshell is a new substitutive method of Watershed transform. The following results are obtained using an Acer Aspire E1 laptop with 8 gb of RAM. The figure 5.1 shows all the process starting from the gray scale image to the mask used to find only the leukocytes. The last two figures 5.2 5.3 show the real result of the segmentation.

As it possible to see, between the two images 5.2 and 5.3 there are some differences. The more visible difference is the bigger presence of agglomerate of small areas that create a kind of cell in the first segmentation. This happened because it was an artefact caused by the Giemsa stain method, but in our approach we can discriminate all this little areas going to remove them because the over-segmentation of this kind (where there are only little areas) means that it is not a leukocyte but only a stain of colour. The result of the counting in this case is 29. Working with cropped images we obtain a better result because we have to analyse less cells and as a consequence we have an increase of the speed as it is explained in the table 5.1. The table shows only the images where is present the worst case of overlap and clump between the cells. The images where is not present any kind of contact between the cells are well segmented with no problem of over-segmentation with an accuracy of 100%. In the images 5.4, 5.5 there is an example of segmentation of six cells without any kind of over-segmentation or division. This is only an example but our implementation works very well with all the images with no overlapped cells.

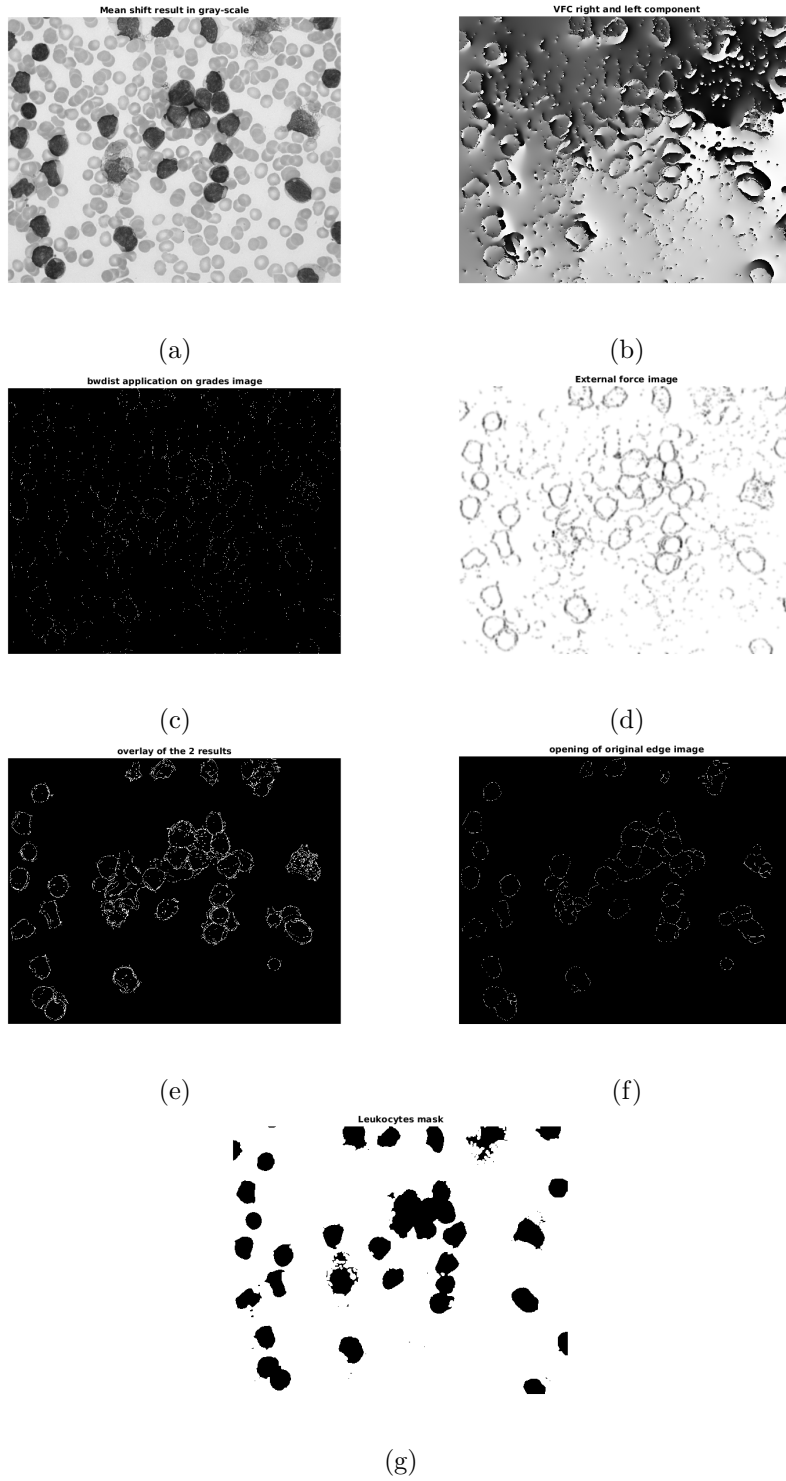


Figure 5.1: (a) Mean shift result in gray scale, (b) VFC u and v components, (c) Distance transform on grades image, (d) External force image, (e) Overlay of two results, (f) Opening of initial edge image, (g) Leukocytes mask

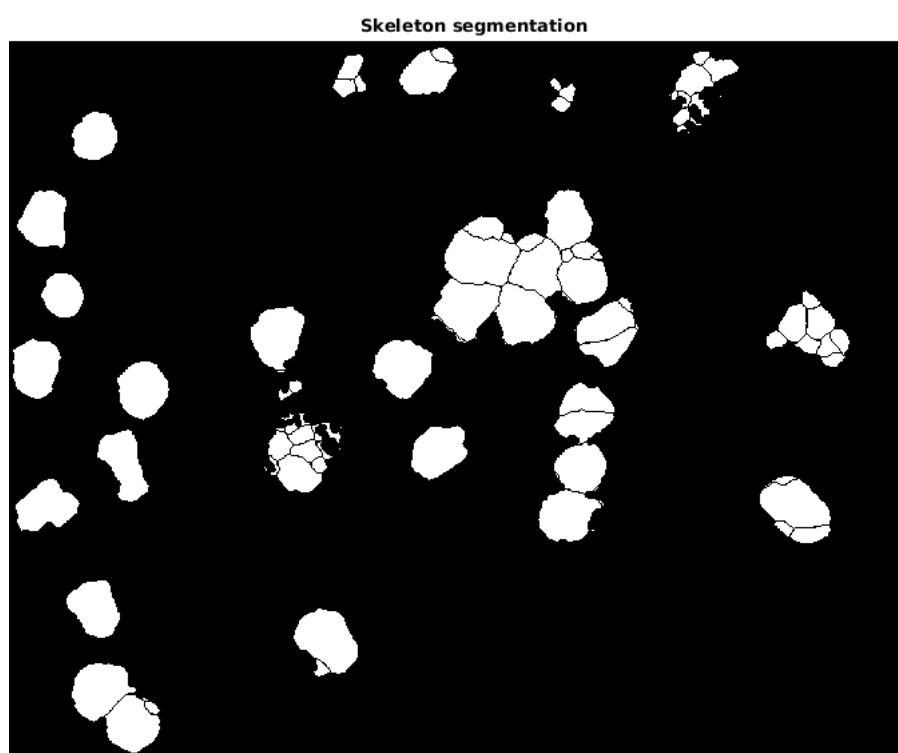


Figure 5.2: Skeleton segmentation

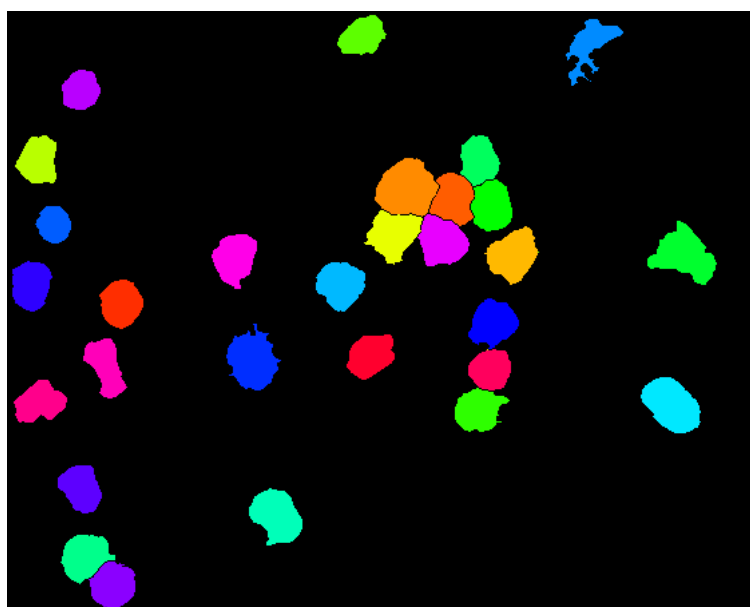


Figure 5.3: Merging of little area to count the number of leukocytes

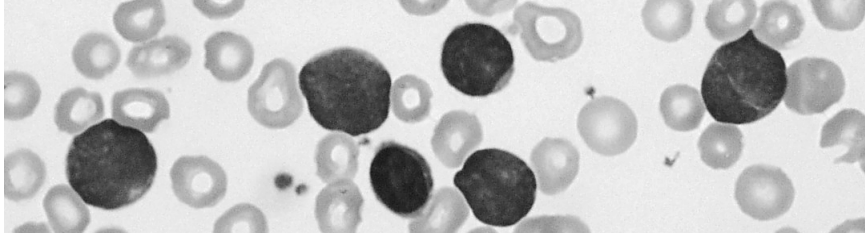


Figure 5.4: Leukocytes after Mean shift application

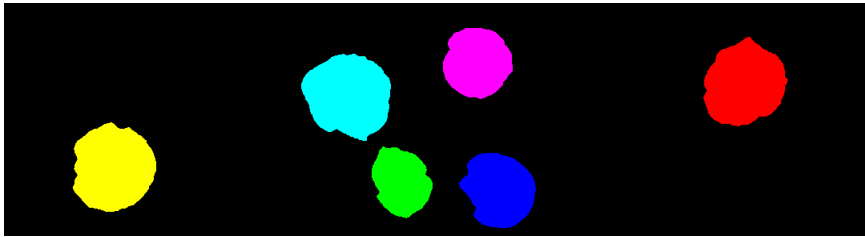


Figure 5.5: Segmented leukocytes

name	cropped	time	Number of recognized cells / number of real cells
image 5	no	45.050214	29/29
image 5	yes	2.214306	7/7
image 13	no	31.827737	11/11
image 13	yes	1.189616	4/4
image 18	no	31.493120	18/17
image 18	yes	1.717642	3/3

Table 5.1: Statistics result

In this case we do not need the mean shift application because the cells are well distant from themselves. This means that the computational cost is very less then the version with the mean shift application (total time < 1 second).

5.2 Related works

Checking the results in presence of clumps or cells overlap, our obtained results are better if we compare them with the results of another work that uses the same dataset [8]. In this work the WBC counting is performed by counting a number of connected components but it is not present a method to divide the clumped cells. We obtain a very close result if we compare our system with a previous work proposed in [3] even though in this work the clumped and the overlapped cells are not well segmented. To evaluate the results, we compared ours with the results obtained in [9] in term of accuracy. Taking a look on the results showed in table 5.2 it is evident that our worst score (86%) is better than the worst result of the related work (55%). In this case the images are composed of significant overlaps between leukocytes, which are difficult to find even for human experts pathologists.

5.3 Conclusions and future works

The dissertation proposed an innovative white blood cell recognition and segmentation system. It was implemented using some notions already known in literature but never applied in this field. Combining them we obtain a new innovative method in which the major innovation is the use of the Vector field convolution in union to the mean shift and the skeleton function to obtain a result better than the watershed method in terms of cells separation from clumps.

The algorithm produces very good results where we analyse images where granulocytes are missing, because the shape of its nucleus produces a not properly segmentation; however we can use it as a base for a detection system

5.6 5.7 The most important points that we focused in this thesis can be listed as follows:

1. preprocessing by using the mean shift algorithm in order to reduce all the differences of colour inside the cells;
2. extrapolation of the right and left component of the VFC force;
3. application of the skeleton in order to separate the overlapped cells;
4. recognize and count of the cells.

number image	accuracy of related system ([9]) (in %)	accuracy of our system (in %)
1	55	100
2	100	83
3	91	100
4	57	86
5	79	100
6	100	86
7	100	100
8	94	94
9	100	100
10	100	100
11	80	100
12	100	94
13	70	100
14	60	100
15	100	100
16	100	95
17	100	100
18	100	93
19	100	91
20	100	100
21	100	100
22	100	100
23	100	100
24	100	100
25	100	100
26	100	100
27	100	100
28	100	100
29	100	100
30	100	100
31	100	100
32	100	100
33	100	100
tot. avg.	90.5	94.6

Table 5.2: Performance of the proposed method for WBCs identification

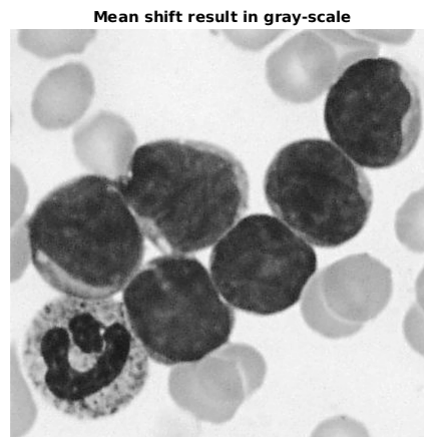


Figure 5.6: Granulocyte after Mean shift application



Figure 5.7: Granulocyte segmentation

Our method demonstrates that, at this moment, it is better than every algorithm existing in literature. The only remaining issues are that it cannot be too robust, due to the low quality of images and the over-segmentation caused by the granulocytes. But as the literature says, this is the complex field in haematological image segmentation.

Future works will include to propose a new kind of region merging algorithm in order to delete all the over-segmentation, an improvement to obtain a better segmentation of granulocytes and a new points-linking function to remove the skeleton side of the algorithm and use only the information given by the VFC components.

List of Figures

1	Example of the different kind of leukocytes[10]	2
1.1	(a) Dipole electric field, (b) Electric dipole	8
4.1	Method diagram representation	24
4.2	(a) Example of two circle in overlap, (b) Distance transform, (c) Watershed result	25
4.3	(a) Original leukocytes image, (b) Watershed transform applied to three cells in overlap	26
4.4	(a) Original image, (b) Mean-shift result, (c) Difference between mean-shift image and original image	28
4.5	Degrees image	29
4.6	Median filter on degrees image	29
4.7	Bwdist applied on degrees image	30
4.8	External energy result	32
4.9	External energy image of leukocytes without red blood cells	32
4.10	Edges and region	32
4.11	Overlay of figures 4.6 and 4.10	33
4.12	Only leukocytes edges	33
4.13	Skeleton of leukocytes with irregular branches	34
4.14	Skeleton of leukocytes with no spurious branches	35
4.15	Final leukocytes segmentation	36
4.16	(a) All the regions, (b) Only big regions	37
4.17	Union of two different areas	38
4.18	Merge of two areas	38
4.19	Union of initial image and new area	38
5.1	(a) Mean shift result in gray scale,(b) VFC u and v components,(c) Distance transform on grades image,(d) External force image,(e) Overlay of two results,(f) Opening of initial edge image,(g) Leukocytes mask	42
5.2	Skeleton segmentation	43
5.3	Merging of little area to count the number of leukocytes	43
5.4	Leukocytes after Mean shift application	44
5.5	Segmented leukocytes	44

5.6	Granulocyte after Mean shift application	47
5.7	Granulocyte segmentation	47

List of Tables

4.1	Characteristics of the dataset. Images acquisition has been performed with a Canon PowerShot G5. Magnification of microscope goes from 300 to 500. The image format of the ALL- IDB1 folder images is JPG, ALL-IDB2 images have TIF format. The colour is 24 bit depth.	26
5.1	Statistics result	44
5.2	Performance of the proposed method for WBCs identification .	46

Bibliography

- [1] Scott T. Bing L. “Active Contour External Force Using Vector Field Convolution for Image Segmentation”. In: *Acton*, vol. 16, pp. 2096 - 2106 (2007) (cit. on p. 20).
- [2] P. Meer D. Comaniciu. “Mean shift: A robust approach toward feature space analysis”. In: *IEEE Transactions on Pattern Analysis and Machine Intelligence*, vol. 24, pp. 603 - 619 (2002) (cit. on p. 15).
- [3] Putzu L. Di Ruberto C. Loddo A. “A Multiple Classifier Learning by Sampling System for White Blood Cells Segmentation”. In: *proceedings in CAIP*, vol. 9257, pp. 415 - 425 (2015) (cit. on p. 45).
- [4] Umbaugh Scott E. “Digital image processing and analysis : human and computer vision applications with CVPitools”. In: *Journal of Electronic Imaging*, pp. 1 - 977 (2010) (cit. on p. 11).
- [5] Woods R. E. Gonzalez R. C. “Digital Image Processing”. In: 2nd ed. *New Jersey: Prentice Hall, Inc.*, pp. 1 - 954 (2002) (cit. on p. 9).
- [6] Fukunaga K. “The estimation of the gradient of a density function, with applications in pattern recognition”. In: *IEEE Transactions on Information Theory*, vol. 21, pp. 32 - 40 (1975) (cit. on p. 15).
- [7] Scotti F. Labati R. D. Piuri V. “ALL-IDB: THE ACUTE LYMPHOBLASTIC LEUKEMIA IMAGE DATABASE FOR IMAGE PROCESSING”. In: *proceedings in Image Processing (ICIP)*, pp. 2045-2048 (2011) (cit. on p. 24).
- [8] Mahasweta J. Joshi Lata A. Bhavnani Udesang K. Jaliya. “Segmentation and Counting of WBCs and RBCs from Microscopic Blood Sample Images”. In: *proceedings in MECS (<http://www.mecspress.org/>)*, vol. 11, pp. 32 - 40 (2016) (cit. on p. 45).
- [9] Di Ruberto C. Putzu L. Caocci G. “Leucocyte classification for leukaemia detection using image processing techniques”. In: *Artificial Intelligence in Medicine*, vol. 62 , pp. 179 - 191 (2014) (cit. on pp. 23, 45, 46).
- [10] Nikhil V. Shubham M. Lalit M. S. “Counting and classification of white blood cell using Artificial Neural Network (ANN)”. In: *proceedings in Power Electronics, Intelligent Control and Energy Systems (ICPEICES)*, pp. 1 - 5 (2017) (cit. on p. 2).

- [11] Unimi. *ALL-IDB Acute Lymphoblastic Leukemia Image Database for Image Processing*. 2005. URL: <https://homes.di.unimi.it/scotti/all/> (cit. on p. 26).
- [12] Wikipedia. *Blood*. 2007. URL: <https://en.wikipedia.org/wiki/Blood> (cit. on p. 1).
- [13] Wikipedia. *Region growing*. 2008. URL: https://en.wikipedia.org/wiki/Region_growing (cit. on p. 10).
- [14] Prince J. L. Xu C. “Generalized gradient vector flow external forces for active contours”. In: *Signal Process.*, vol. 71, pp. 131 - 139 (1998) (cit. on p. 19).
- [15] Cheng Y. “Mean shift, mode seeking, and clustering”. In: *IEEE Transactions on Pattern Analysis and Machine Intelligence*, vol. 17, pp. 790 - 799 (1995) (cit. on p. 15).